

Manuscript Number: SAMES-D-16-00150R1

Title: The development of Miocene extensional and short-lived basin in the Andean broken foreland: the Conglomerado Los Patos, Northwestern Argentina

Article Type: Research Paper

Keywords: alluvial sedimentation, Andean foreland, NW Argentine, Puna

Corresponding Author: Dr. Cecilia del Papa, Ph.D.

Corresponding Author's Institution: CONICET

First Author: Cecilia del Papa, Ph.D.

Order of Authors: Cecilia del Papa, Ph.D.; Ivan Petrinovic

Abstract: The Conglomerado Los Patos is a coarse-grained clastic unit that crops out irregularly in the San Antonio de los Cobres Valley in the Puna, Northwestern Argentina. It covers different units of the Cretaceous-Paleogene Salta Group by means of an angular unconformity and, in turn, is overlaid in angular unconformity by the Viscachayoc Ignimbrite (13 ± 0.3 Ma) or by late Miocene tuffs.

Three lithofacies have been identified in the Corte Blanco locality; 1) Bouldery matrix-supported conglomerate (Gmm); 2) Clast-supported conglomerate (Gch) and 3) Imbricated clast-supported conglomerate (Gci). The stratigraphic pattern displays a general fining upward trend. The sedimentary facies association suggests gravitational flow processes and sedimentation in alluvial fan settings, from proximal to medial fan positions, together with a slope decrease upsection. Provenance studies reveal sediments sourced from Precambrian to Ordovician units located to the southwest, except for volcanic clasts in the Gmm facies that shows U/Pb age of 14.5 ± 0.5 Ma. This new age represents the maximum depositional age for the Conglomerado Los Patos, and it documents that deposition took place simultaneously during a period of increased tectonic and volcanic activity in the area.

The structural analysis of the San Antonio de los Cobres Valley and the available thermochronological ages, indicate active N-S main thrusts and NW-SE transpressive and locally normal faults during the middle Miocene. In this context, we interpret the Conglomerado Los Patos to represent sedimentation in a small, extensional and short-lived basin associated with the compressional Andean setting.

**The development of Miocene extensional and short-lived basin in the Andean
broken foreland: the Conglomerado Los Patos, Northwestern Argentina**

Cecilia E. del PAPA* e Ivan A. PETRINOVIC*

*CICTERRA -Facultad de Ciencias Exactas, Físicas y Naturales, Universidad Nacional
de Córdoba, Av. Vélez Sarsfield 1611, X5016GCA, Córdoba, Argentina

Corresponding author: ceciliadelpapa@unc.edu.ar

19 pages, 1 table, 7 figures

1
2
3
4
5
6
7
8
9
10
11
12
13
14
15
16
17
18
19
20
21
22
23
24
25
26
27
28
29
30
31
32
33
34
35
36
37
38
39
40
41
42
43
44
45
46
47
48
49
50
51
52
53
54
55
56
57
58
59
60
61
62
63
64
65

Abstract

The Conglomerado Los Patos is a coarse-grained clastic unit that crops out irregularly in the San Antonio de los Cobres Valley in the Puna, Northwestern Argentina. It covers different units of the Cretaceous-Paleogene Salta Group by means of an angular unconformity and, in turn, is overlaid in angular unconformity by the Viscachayoc Ignimbrite (13 ± 0.3 Ma) or by late Miocene tuffs.

Three lithofacies have been identified in the Corte Blanco locality; 1) Bouldery matrix-supported conglomerate (Gmm); 2) Clast-supported conglomerate (Gch) and 3) Imbricated clast-supported conglomerate (Gci). The stratigraphic pattern displays a general fining upward trend. The sedimentary facies association suggests gravitational flow processes and sedimentation in alluvial fan settings, from proximal to medial fan positions, together with a slope decrease upsection. Provenance studies reveal sediments sourced from Precambrian to Ordovician units located to the southwest, except for volcanic clasts in the Gmm facies that shows U/Pb age of 14.5 ± 0.5 Ma. This new age represents the maximum depositional age for the Conglomerado Los Patos, and it documents that deposition took place simultaneously during a period of increased tectonic and volcanic activity in the area.

The structural analysis of the San Antonio de los Cobres Valley and the available thermochronological ages, indicate active N-S main thrusts and NW-SE transpressive and locally normal faults during the middle Miocene. In this context, we interpret the Conglomerado Los Patos to represent sedimentation in a small, extensional and short-lived basin associated with the compressional Andean setting.

Key words: alluvial sedimentation, Andean foreland, Northwestern Argentina, Puna

1. Introduction

In recent years, several contributions have improved the knowledge of the Andean foreland system in the northwestern Argentina. In particular, research has developed new insights and concepts on tectonics, sedimentation and volcanism (Coutand et al., 2001; Carrapa et al., 2005; Petrinovic et al., 2006; Hongn et al., 2007; Strecker et al., 2007; Mazzuoli et al., 2008; Folkes et al., 2011; Guzmán et al., 2011; del Papa et al., 2013; Canavan et al., 2014). The most important improvements include: the existence of an Eocene broken foreland basin in the Puna and in the Eastern Cordillera, the role of

1 the inversion of the Cretaceous normal faults and basement heterogeneities in the
2 deformation and in the generation of the double vergence structures, the existence of
3 orogen-oblique transfer zones between double vergence master thrusts, the presence of
4 Eocene growth-strata in the continental hinterland, and the increment of Paleogene and
5 early Miocene ages of uplift and exhumation data (Carrapa and DeCelles, 2008; Payrola
6 et al., 2009; Carrapa et al., 2011; Hongn et al., 2011; del Papa et al., 2013). The
7 described scenario suggests the hypothesis that isolated basins -connected or
8 disconnected- developed, with distinct evolutions. Thus, the new challenge in
9 Northwest Argentina is to recognize and differentiate these basins, and also to interpret
10 their tectono-stratigraphic signature in the context of the complex foreland system.
11
12
13
14
15
16
17
18

19 The Conglomerado Los Patos is a clastic sedimentary unit that crops out near the village
20 of San Antonio de los Cobres, close to the eastern border of the Puna (Fig. 1). There are
21 no previous detailed studies of this unit, which is most likely due to its discontinued,
22 isolated outcrops and its low preserved thickness. Nevertheless, its position on the
23 border of the Puna, its stratigraphic relationships, and particular features of the
24 sediments suggest the Conglomerado Los Patos is a key unit to understanding the
25 evolution of these foreland basins and the Miocene configuration along the Eastern
26 Puna margin.
27
28
29
30
31
32
33

34 In this contribution, we present stratigraphic and sedimentological studies and new
35 radiometric ages from volcanic clasts of the Conglomerado Los Patos. These new data
36 integrate with a structural analysis of the area allow for a discussion of the formation of
37 extensional short-lived basins in the compressional orogenic Andean setting.
38
39
40
41
42

43 **2. Geological background**

44

45 The Conglomerado Los Patos was first mentioned by Ramos (1973) as a fanglomeratic
46 unit cropping out along the margins of the Los Patos River and in the Angosto de
47 Piscuno, near San Antonio de los Cobres (Fig.1). This author described it from the base
48 to the top, as integrated by red mudstones, coarse-grained sandstones and grayish white
49 conglomerate rocks deposited in angular unconformity over the Cretaceous-Paleogene
50 Salta Group. Donato and Vergani (1988) confirmed the angular unconformity relation
51 with the Salta Group and described the Conglomerado Los Patos as mainly integrated
52 by a polymictic orthoconglomerate deposited in alluvial fan setting.
53
54
55
56
57
58
59
60
61
62
63
64
65

Figure 1

3. Regional distribution and stratigraphy

The Conglomerado Los Patos crops out in a narrow longitudinal belt between the Angosto de Piscuno to the north (Ramos, 1973) and the Abra del Acay to the south (Fig. 1 A; B). Outside this belt, there are no deposits that can be attributed to the Conglomerado Los Patos. It lays in angular unconformity over the Santa Bárbara Subgroup – Salta Group, Fig. 2. In the Corte Blanco locality, along the train tracks, the base of the Conglomerado Los Patos lies by angular unconformity over Mealla (Me), and laterally over Maíz Gordo (MG) and Lumbrera formations of the Santa Bárbara Subgroup (Fig. 2 A; B). The basal contact is a very irregular erosional surface that, in some places, forms high relief gullies (Fig. 2 C). Moreover, along the unconformity surface, the units of the Salta Group show decolorization and brecciation, attesting to a weathering paleosurface (Fig. 2 B). The upper contact surface is an irregular unconformity, that is partly sealed by the pyroclastic deposits of the Viscachayoc Ignimbrite (Fig. 2 D) and/or by the Toba I pyroclastic rocks (Viramonte et al., 1984). This erosive surface is also marked by a lateral thinning up to the complete absence of the Conglomerado Los Patos (Fig. 2 A).

Figure 2

4. Sedimentology

The thickness measured in the Corte Blanco locality is 15 meters (Fig. 3), but laterally it reaches more than 40 meters. Ramos (1973) mentions thicknesses of up to 270 meters. The Conglomerado Los Patos is characteristically yellowish brown and shows a fining and thinning upward patterns, from boulder to pebble size deposits.

Figure 3

We recognized three lithofacies

a) **Matrix supported bouldery conglomerate** (Gmm). This facies is in the lower part of the unit and consists of very thick strata (up to 2 m) with crude stratification. The beds are reddish brown, with lenticular, cuneiform or tabular geometries (Fig. 4A). The clasts are boulder (~0.6 m) and cobble size, angular to subrounded, disorganized, ungraded, except for one level with inverse grading (Gmig), floating in a fine-grained

1 sandy mudstone to wacke matrix (Fig. 4 A and B). Conglomerate clasts are composed
2 of low to medium grade metamorphic (phyllites, schist), quartz-arenite, porphyritic
3 rhyolite and pyroclastic rocks (Fig. 4 B and C). The porphyritic rhyolite is rich in
4 tourmaline phenocrysts. The pyroclastic clasts are whitish in color and composed of a
5 coarse-grained ash (Fig. 4 B), subrounded pumice fragments with biotite,
6
7 clinopyroxene, hornblende and plagioclase phenocrysts and angular lithic fragments of
8
9 meta-pelites and quartz-arenites.
10

11
12
13 The sedimentological characteristics suggest deposition by frictional freezing from
14 cohesive debris flows (Nemec and Steel, 1984). The inverse grading level suggests
15 debris flows with high dispersive pressure mechanism, also favored by the presence of
16 boulder-sized clasts (Costa, 1984).
17
18
19
20

21
22 **b) Clasts supported conglomerate** (Gch). This facies consists of 40-50 cm thick beds,
23 vertically stacked up to 4 m thick, with crude stratification (Fig. 4 D). It is integrated by
24 pairs of cobble-rich levels at the base and pebble-rich levels at the top (Fig. 4 E).
25

26
27 Internally, it shows clast supported fabric without grading; clasts are subangular to
28 subrounded, elongated/flat clasts accommodated parallel to stratification. The matrix is
29 composed of fine-grained muddy sandstones.
30

31
32 This facies represents deposition from gravitational non-cohesive flows (Blair and
33 McPherson, 1994). These flows are produced from catastrophic discharges of water,
34 where water-sediment mixture is able to transport coarse material by dispersive and
35 buoyant forces with low mud participation (Blair and McPherson, 2009). This is a
36 common process in high relief apical zones of alluvial fans.
37
38
39
40
41

42
43 **c) Imbricated conglomerate** (Gci). It is made up of 20-30 cm thick stacked tabular
44 beds of yellowish-brown pebbly conglomerate. Conglomerate is clast-supported with
45 slight normal grading; clasts are subrounded and less frequently, subangular, elongated
46 and flat shapes are parallel to the stratification and present well-developed imbrication
47 (Fig. 4 F). This facies displays low proportion of matrix, of silt/sand fractions.
48

49
50 This facies is interpreted to be deposited by clast-rich, turbulent and unconfined flows,
51 of sheet-flood type, which are common after heavy rains (Blair and McPherson, 1994;
52 Blair, 1999; Jan and Cooker, 2016).
53
54
55
56

57 Figure 4

58 59 **4.1. Paleoenvironment** 60 61 62 63 64 65

1 The sedimentary facies and the interpreted processes are dominated, in all cases, by a
2 gravitational component. This is typical of high relief environment such as mid-to-
3 proximal alluvial fan settings. The irregular geometries of the cohesive debris flow
4 deposits (Gmm) suggest the infill of paleochannels and gullies until the complete infill
5 smooth the paleotopography. These characteristics are consistent with the infill of
6 incised feeder channels in proximal to apical zones in alluvial fan settings (Blair and
7 McPherson, 1994). The younger sedimentary processes were dominated by unconfined
8 sheet-flood that produced tabular units, suggesting mid-to-proximal positions in the fan
9 lobes (Blair and McPherson, 2009).

10
11
12
13
14
15
16
17 The vertical sedimentary pattern, in combination with the confined cohesive flow in the
18 lower section which shifts to unconfined dilute flows in the upper section, indicates an
19 aggradational to retrogradational system that is consistent with the local decreasing
20 paleo-slope (Fraser and DeCelles, 1992).

21 22 23 24 25 **5. Age and Provenance of the Conglomerado Los Patos**

26
27 We carried out two new age determinations from both porphyritic and pyroclastic clasts
28 included in Gmm facies to gain information on the age of the Conglomerado Los Patos.
29 The two new U/Pb radiometric ages in zircons, were performed in the Geochronology
30 Laboratory of the Brasilia University, on a LAM-HR-ICPMS (Neptune) equipped with
31 9 Faraday detectors, a multiplier central electrons to 5 meters ions coupled to a LA Nd-
32 YAG 213 NewWave. The first radiometric age performed in porphyritic rhyolites clast
33 results in (concordia) 483 ± 10 Ma (U/Pb), (Fig. 5 A). The second U/Pb radiometric
34 analysis in zircons was carried out from a pumice fragment included in a pyroclastic
35 clast located at few centimeters from the base of the unit (Fig. 3). The new age is $14.5 \pm$
36 0.5 Ma. (see Fig. 5 B for details). Taking into account this 14.5 ± 0.5 Ma age of the
37 lower clast and the 13 ± 0.3 Ma age in the Viscachayoc Ignimbrite (Petrinovic et al.,
38 1999), the age of the Conglomerado Los Patos is constrained between 14.5 ± 0.5 Ma
39 and 13 ± 0.3 Ma.

40 41 42 43 44 45 46 47 48 49 50 51 52 53 **Figure 5**

54
55 The clast compositions in the lower section of the Conglomerado Los Patos are of
56 schist, phyllite, meta-pelite, porphyritic rhyolite and pyroclastic rocks (Fig. 3).
57 Upsection, both porphyritic and pyroclastic rocks completely disappear and the main
58
59
60
61
62
63
64
65

1 component is meta-pelites (40%) followed by phyllites, micaceous schist, quartz arenite
2 and porphyritic rhyolite (Fig. 3).
3

4 The lithology of the metamorphic and plutonic clasts agrees with the local basement,
5 which is formed by low-grade metamorphic Puncoviscana Formation (Turner, 1960)
6 and Ordovician sedimentary and plutonic rocks of the Faja Eruptiva Oriental (Méndez
7 et al., 1973) and/or the Oire Eruptive Complex (Blasco et al., 1996). All these units crop
8 out in the surrounding area (Fig. 1). The first acquired Ordovician radiometric age
9 confirms its provenance (Fig. 5 A). Rocks with similar composition have been described
10 in the Organullo and Cajón creeks toward the SW of the study area (Fig. 1), interbedded
11 in the clastic sedimentary succession of Ordovician age (Suzaño et al., 2015).
12
13
14
15
16
17
18
19

20 On the other hand, the provenance of the middle Miocene pyroclastic clasts is uncertain.
21 There are no known equivalent ages in the proximities of the Corte Blanco outcrop.
22 However, extended lava domes and related deposits, which remain undated, are exposed
23 in the Rupasca complex (Fig. 1). Hence, we speculate that the provenance of these
24 pyroclastic clasts may be from Rupasca, which is located 30 km toward the SW.
25
26
27
28
29

30 The upper section of the Conglomerado Los Patos is integrated by Gci facies that
31 allowed paleoflow determination from imbricated clasts. The paleoflow analysis reveals
32 currents toward the N-NE (Fig. 3). This direction agrees with the composition of the
33 described detrital material and with the potential source areas.
34
35
36
37

38 **6. The structural framework of the San Antonio Valley**

39

40 In order to gain into the knowledge of the structural framework, we analyzed the
41 available information from Ramos (1973), Marrett et al. (1994), Donato and Vergani
42 (1988), Blasco et al. (1996), Gangui and Götze (1996), Riller et al (2001), Seggiaro
43 (2006), Petrinovic et al. (2010), Santimano and Riller (2012), Salado Paz et al. (2016)
44 and added new information from seven stations (Fig. 1 A), shown in the dataset of
45 Table 1.
46
47
48
49
50

51 Table 1
52
53
54

55 The San Antonio de los Cobres Valley is limited by approximately N-S striking, reverse
56 faults with opposite vergence (Fig. 1 A). The double- vergency of the structures is a
57 common feature of the Andean deformation in the Puna-Eastern Cordillera transition. It
58
59
60
61
62
63
64
65

1 has been interpreted to be controlled by the presence of previous heterogeneities in the
2 upper crust (Hongn et al., 2010). From the west to the east the major faults are: the east
3 vergence “West Salinas Grandes Thrust” (WSGT: Gangui and Götze, 1996) and its
4 continuation in the Charco and Cajón thrusts and, the west vergence Muñano Fault (Fig.
5 1 A). The WSGT and the Muñano faults thrust the Precambrian and Ordovician rocks
6 over the sediments of the Salta Group and over Neogene volcanic/sedimentary
7 successions (Donato and Vergani, 1988; Gangui and Götze, 1996). The WSGF is, at
8 least, of Miocene-Pliocene age (Schwab and Lippot, 1974), meanwhile the Muñano
9 Fault and its conjugated planes, displace and fold volcano-sedimentary successions of
10 late Miocene-Pliocene age (Donato and Vergani, 1988).

11
12
13
14
15
16
17
18
19 Towards the south, the valley is closed by a topographic high of ~1500 meters and to
20 the north, by the active fluvial system draining to the Salinas Grandes playa-lake (Fig. 1
21 A). Numerous fault planes and small-scale folds cut the valley floor that are parallel and
22 oblique (Fig. 1 A) to the strike of the main faults (Donato and Vergani, 1988; Marrett et
23 al., 1994; Gangui and Götze, 1996; Seggiaro, 2006).

24
25
26
27
28
29 Near the Nevado de Acay (Fig. 1 A), the Muñano Fault uplifts Precambrian basement
30 rocks over Salta Group sediments (Fig. 6 A) and is, in turn, covered by lava flows from
31 the Negra Muerta volcanic complex, dated 7.4 Ma (Petrinovic et al., 2005). The trace of
32 the Muñano Fault continues to the south in the high angle Calchaquí Fault (Fig. 1 A)
33 that uplifted the Puncoviscana Formation over the Salta Group and over Andean
34 orogenic sediments. The Calchaquí Fault shows evidence of activity from the middle
35 Eocene (Hongn et al., 2007) to the present day (Santimano and Riller, 2012).

36
37
38
39
40
41
42
43 In the inner area of the San Antonio de los Cobres Valley, several minor order faults
44 with NW strike and folds with N-NE axis directions (Fig. 1 A) affected the Salta Group
45 sediments and younger volcanic rocks (Donato and Vergani, 1988). On the other hand,
46 the Cajón Fault thrusts Ordovician granitoids over sediments of the Salta Group (Fig. 1
47 A). The N-S and low angle fault plane (Fig. 1 A and Table 1) displays a 10 meter wide
48 brecciated zone that mainly affects conglomerates of the Pirgua Subgroup (Fig. 6 B). Its
49 northward prolongation is the Western Charco Fault (Fig. 1 A), which also uplifted
50 granitoids over the Salta Group, with the same characteristics. The fault plane presents
51 *ca.* 45° angle (Fig. 6 C and Fig. 1 A) and predates the 13 +/- 0.2 Ma (JICA 1993)
52 Concordia volcanic center (Fig. 1).

Figure 6

The Eastern Charco Fault uplifts Precambrian and Ordovician sediments over the Salta Group through high to moderate angle fault plane (Fig. 1 A). Both faults (Western and Eastern Charco) limit a narrow bivergent valley that controls the Concordia volcanic center emplacement and its mineralization (Petrinovic et al., 2010). This complex fault system continues to the north in the WSGF, which limits the western border of the Salinas Grandes, as observed in seismic profiles (Gangui and Götze, 1996).

To the south, the Pastos Grandes fault thrusts basement rocks over the Eocene to Miocene sediments with west-vergence (Fig. 1 A) and shows a vertical offset of hundreds to thousand meters. This master fault system quickly loses entity northwards, until it reaches the Calama-Olacapato-El Toro (COT) fault system (Fig. 1 A).

The Toro Muerto Fault, that limits the western side of the heads of the Calchaquí Valley (Fig. 1 A), represents a series of east-vergence fault planes that uplift the Precambrian and Ordovician rocks over the Salta Group (Fig. 6 D) with variable dip (Hongn et al., 2010). This fault attenuates towards the north, close to the Nevado de Acay zone, probably due to dissipation in NW and E-W transfer faults with normal to left lateral strike-slip component in the Saladillo Fault (Fig. 1 A). Parallel fault planes with similar characteristics control the emplacement of the Negra Muerta volcanic vents (Riller et al., 2001).

The Calchaquí Fault (Fig. 1 A) is a west-vergence, high angle thrust that uplifts Precambrian basement and provoke drag folds in the Salta Group (Donato and Vergani, 1988, Hongn et al., 2007). To the north, it continues as the Muñano Fault (Fig. 1 A) with similar characteristics. The emplacement of the 12.6 ± 0.3 Ma Nevado de Acay Granite along this fault-plane, plus the low-temperature thermochronological data (Insel et al., 2012) attests the syntectonic character of the intrusion. Several minor order faults oblique to the Calchaquí Fault and parallel to the Saladillo Fault (Fig. 1 A) are interpreted as conjugated and transfer faults in the northern Calchaquí Valley (Riller et al., 1999). Our data on the NW prolongation of the Saladillo fault planes (Fig. 1 A) and those from the Acazoque fault planes (Salado Paz et al., 2016) confirm the oblique (normal to left lateral) component (Table 1 and Fig. 1 A) of this fault.

1 The morphological connection between the northern Calchaquí Valley and the San
2 Antonio de los Cobres Valley occurs through a NW trending belt that forms a
3 topographic high (~ 1500 m) from Saladillo to Rupasca-Organullo (Fig. 1 A and DEM of
4 Fig. 7). This belt is composed of Precambrian basement and Ordovician rocks (Blasco
5 et al., 1996) covered by middle Miocene lava flows and pyroclastic deposits (Petrinovic
6 et al., 1999). Interestingly, this belt is highlighted by the absence of Salta Group
7 sediments.
8
9
10
11
12

13 **7. Interpretation and discussion**

14
15

16 The Conglomerado Los Patos represents the clastic accumulation in alluvial fan setting
17 developed at the foot of a paleo-topographic break (Donato and Vergani, 1988). The
18 composition of the clasts and paleoflows indicate provenance from the south-southwest,
19 suggesting the drainage area and rock sources in these directions. Despite the fact, the
20 Conglomerado Los Patos is always overlaying the Salta Group rocks; we did not
21 recognize clastic components ascribable to these deposits, suggesting that this
22 sedimentary unit did not integrate the drainage area. Instead, the source areas are
23 composed of Precambrian- early Paleozoic units, with subordinated participation of
24 Miocene volcanic rocks (Fig. 3). At present day, these units crop out in a 4000-4500 m
25 range that divides the San Antonio de los Cobres Valley to the N, the Pastos Grandes-
26 Centenario Valley to the SW, and the Calchaquí Valley to the SSE (Figs. 1 A; 7 A).
27 These three valleys are limited by west-vergence and east-vergence reverse faults, with
28 evidence of fault activity controlling basin configuration since the Paleogene (del Papa
29 et al., 2013). The absence of Salta Group rocks as detritus sources confirm the early
30 activity of faults, as was previously shown in Cretaceous paleogeographic
31 reconstructions (Salfity et al., 1984). This indicates that the Salta basin was developed
32 eastwards and northwards of the Pastos Grandes ranges and the COT fault system (Fig.
33 7; from now COT).
34
35
36
37
38
39
40
41
42
43
44
45
46
47
48
49

50 Figure 7

51
52 Contrary to the expected “typical” sedimentary pattern in alluvial fans progradation
53 systems related to continuous uplift of the source areas (Frazer and DeCelles, 1992), the
54 sedimentary facies succession that evolves from cohesive debris flows to dilute flows
55 and the decreasing grain-sizes suggest the retraction of the topographic gradient (Blair
56 and McPherson, 1994; Frazer and DeCelles, 1992). The stratigraphic pattern, along with
57
58
59
60
61
62
63
64
65

1 the restricted distribution of the Conglomerado Los Patos, displays characteristics of
2 extensional basins (e.g. Davila and Astini, 2003). Importantly, this unit crops out in the
3 intersection zone between major N-S faults, such as the Calchaquí-Muñano, Pastos
4 Grandes-Cajón-Charco faults and the NW-SE COT (Fig. 1 A).
5
6

7
8 COT activity predates the Andean cycle. The absence of Salta Group sediments to the
9 SW of the COT in the Puna (Fig. 1 A) has been interpreted as a normal rift fault dipping
10 to the north (Seggiaro, 2006). This interpretation agrees with the Cretaceous and post-
11 Cretaceous paleogeographic reconstructions and explains the presence of a highly
12 fractured crustal zone along the COT (Fig. 7). Additionally, the recent 107.6 Ma ZHe
13 age determination has confirmed the Cretaceous thermal cooling and exhumation event
14 (Reiners et al., 2015).
15
16
17
18
19
20

21 The extensional character of the COT has been well documented by previous
22 kinematical analyses in the region (e.g. Fig. 4 in: Riller and Oncken 2003). Riller et al.
23 (2001) interpreted normal faults close to the intersection between the COT with the
24 Calchaquí Fault trace and a NW-SE which are, in turn, the favored planes for the
25 volcanic rocks emplacement of the Miocene Negra Muerta volcanic center. Petrinovic et
26 al. (2005) interpreted a transfer zone with NE normal faults westward of the San
27 Antonio Valley, in the Pleistocene Tocomar volcanic center. Lanza et al. (2013)
28 interpreted it in the same way, extensional components along the COT, while Norini et
29 al. (2013) proposed local extension near San Antonio de los Cobres village. Close to the
30 Cajón fault (Fig. 1A), minor fault planes related with the early Miocene Aguas
31 Calientes caldera has oblique (normal-dextral) relative displacement of blocks (Salado
32 Paz et al., 2016).
33
34
35
36
37
38
39
40
41
42
43

44 At a regional scale, most of the master N-S fault planes are not continuous north and
45 southward from the COT fault system (Figs. 1 A and 7).
46
47
48

49 At a mesoscale structural analysis, our data and the kinematic analyses in both
50 intersections of the COT with the Cajón and Toro Muerto faults (Fig. 1 A) reinforce
51 NE-SW and E-W extensional component of the COT in the San Antonio de los Cobres
52 segment (Fig. 7). The dilation zones in strike-slip systems act as potential
53 accommodation space for sediments storage (Allen and Allen, 1995; Reijs and McClay,
54 1998). Furthermore, in broken foreland systems -such as the Argentinean northwestern
55
56
57
58
59
60
61
62
63
64
65

1 one- it is common that the vergence of the major faults changes along their trace, and
2 locally involves strike-slip components (Jordan, 1995, pp. 360 and references therein).
3 The integration of the sedimentological data and the regional and mesoscale structural
4 information, leads us to propose that during the middle Miocene, the horizontal
5 extension related to the COT fault system activity favored the formation of the
6 accommodation space for Conglomerado Los Patos deposition.
7
8
9

10
11 The brief life period (14.5 ± 0.5 Ma to 13 ± 0.3 Ma) of the Conglomerado Los Patos
12 basin correlates with a period of shortening and uplift in the area. The available AFT
13 thermochronological ages constrain a rapid middle Miocene tectonic uplift. In the study
14 area, the uplift of the Cachi granite is dated at 15 Ma and the Oire Eruptive Complex at
15 16 - 17 Ma (Deeken et al. 2006). The intrusion of Las Burras monzogranite at 14.4 Ma
16 (Hongn et al., 2002) and the collapse of the Cerro Aguas Calientes caldera, at 17.5 Ma
17 (Petrinovic et al., 2010) occurred coeval with the structuration of the eastern border of
18 the Puna. In the same way, the Nevado de Acay monzonite (Llambías et al., 1985) of
19 12.61 ± 0.25 Ma, displays a rapid exhumation age (Insel et al., 2012). The new age of
20 14.5 ± 0.5 Ma presented here represents the maximum depositional age for the
21 Conglomerado Los Patos, and the top is limited by the 13 ± 0.3 Ma Viscachayoc
22 Ignimbrite (Petrinovic et al., 1999). Consequently, the basin formation was
23 contemporaneous with the maximum period of shorting and uplift in the region.
24
25
26
27
28
29
30
31
32
33
34
35

36 Although data is limited due to the occasional exposition of the Conglomerado Los
37 Patos, the data presented here, in combination with data from other research, is
38 consistent and suggest the development of a local, extensional and short- lived basin
39 developed between *ca.* 14.5 and 13 Ma in a regional transpressive setting (Fig. 7).
40 Nevertheless, further detailed structural studies are needed to define the complete
41 geometry of the basin. The Conglomerado Los Patos represents the remnant deposits of
42 this basin and spatially confined to the Corte Blanco-Los Patos depocenter in the San
43 Antonio de los Cobres Valley. The southward limit of the basin was the Precambrian –
44 early Paleozoic block that today forms the Pastos Grandes Range (Cerro Áspero and
45 Abra de Acay: Fig. 1A), which sourced the detritus to the basin. The subsequent events
46 of deformation uplifted and folded the Conglomerado Los Patos, producing its
47 dismemberment and partial suppression.
48
49
50
51
52
53
54
55
56
57
58

59 **Acknowledgements**

60
61
62
63
64
65

1 This research was partially funded by CONICET and FONCyT-ANPCyT (PICT-0407).
2 We kindly thank Silvina Guzmán for useful suggestions on an early version. We also
3 thank to Wendy Walker for revising the English. Two anonymous reviewers are thanked
4 for their constructive comments and Victor Ramos for editorial handling.
5
6

7 **References**

- 8
9
10 Allen, P.A. Allen, J.R., 1995. Basin Analysis, Principles and Applications. Blackwell
11 Publishing, 2° Edition, pp 549.
12
13 Arnosio, J.M., 2002. Volcanismo, Geoquímica y Petrología del volcán Chimpa (24° LS
14 - 66° LO), provincia de Salta, República Argentina. Ph.D. thesis, Facultad de Ciencias
15 Naturales, Salta University.
16
17 Blair, T.C., 1999. Sedimentology of the debris-flow-dominated Warm Spring Canyon
18 alluvial fan, Death Valley, California. *Sedimentology*, 46, 941-965.
19
20 Blair, T.C., McPherson, J.G., 1994. Alluvial fans and their natural distinction from
21 rivers based on morphology, hydraulic processes, sedimentary processes, and facies.
22 *Journal of Sedimentary Research*, A 64, 451-190.
23
24 Blair, T.C., McPherson, J.G., 2009. Processes and Forms of Alluvial Fans. In: A.J.
25 Parsons, A.D. Abrahams (eds.), *Geomorphology of Desert Environments*. Springer
26 Science, 2nd ed., DOI 10.1007/978-1-4020-5719-9J4, 443- 465.
27
28 Blasco, G., Zappettini, E.O., Hongn, F.D., 1996. Hoja Geológica 2566-II, San Antonio
29 de los Cobres, 1:250.000. Secretaría de Minería de la Nación. Bulletin 217. Buenos
30 Aires.
31
32 Canavan, R. R., Carrapa, B., Clementz, M. T., Quade, J., DeCelles, P. G, Schoenbohm,
33 L., 2014. Early Cenozoic uplift of the Puna Plateau, Central Andes, based on stable
34 isotope paleoaltimetry of hydrated volcanic glass. *Geology*, doi:10.1130/G35239.1.
35
36 Carrapa, B., Adelman, D., Hilley, G., Mortimer, E., Sobel, E., Strecker, M., 2005.
37 Oligocene range uplift and development of plateau morphology in the southern central
38 Andes: *Tectonics*, 24, TC4011, doi:10.1029/2004TC001762.
39
40 Carrapa, B., Trimble, J., Stockli, D., 2011. Patterns and timing of exhumation and
41 deformation in the Eastern Cordillera of NW Argentina revealed by (U-Th)/He
42 thermochronology. *Tectonics*, 30, TC3003, doi:10.1029/2010TC002707.
43
44 Carrapa, B., DeCelles, P., 2008. Eocene exhumation and basin development in the Puna
45 of northwestern Argentina. *Tectonics*, 27, TC1015 doi:10.1029/2007TC002127.
46
47
48
49
50
51
52
53
54
55
56
57
58
59
60
61
62
63
64
65

1
2
3
4
5
6
7
8
9
10
11
12
13
14
15
16
17
18
19
20
21
22
23
24
25
26
27
28
29
30
31
32
33
34
35
36
37
38
39
40
41
42
43
44
45
46
47
48
49
50
51
52
53
54
55
56
57
58
59
60
61
62
63
64
65

Coutand, I., Cobbold, P., de Urreiztieta, M., Gautier, P., Chauvin, A., Gapais, D.,
Rossello, E., López Gamundi, O., 2001. Style and history of Andean deformation, Puna
plateau, northwestern Argentina. *Tectonics*, 20 (2), 210-234.

Costa, J.E, 1984. Physical Geomorphology of Debris Flows. In: J.E.Costa & P.J.
Fleisher (Eds), *Developments and Applications in Geomorphology*. Springer-Verlag
Berlin Heidelberg, 268-317.

Dávila, F., Astini, A., 2003. Early Middle Miocene Broken foreland development in the
southern Central Andes: evidence for extension prior to regional shortening. *Basin
Research*, 15, 379-396.

Deeken, A., Sobel, E., Coutand, I., Haschke, M., Riller, U., Strecker, M., 2006.
Development of the Southern Eastern Cordillera, NW Argentina, constrained by apatite
fission track thermochronology: From Early Cretaceous extension to middle Miocene
shortening. *Tectonics* 25, TC6003, doi: 10.1029/2005TC001894.

del Papa, C., Hongn, F., Powell, J., Payrola, P., Do Campo, M., Strecker, M.,
Petrinovic, I., Schmitt, A., Pereyra, R., 2013. Middle Eocene-Oligocene broken-
foreland evolution in the Andean Calchaquí Valley, NW Argentina: insights from
stratigraphic, structural and provenance studies. *Basin Research*, 25, 574-593.

Donato, E., Vergani, G. 1988. Geología del área de San Antonio de los Cobres. *Boletín
Informaciones Petroleras*, 5(15), 83-101. Buenos Aires.

Folkes, C.B. de Silva, Sh., Schmitt, A.K., Cas, R., 2011. A reconnaissance of U-Pb
zircon ages in the Cerro Galán system, NW Argentina: Prolonged magma residence,
crystal recycling, and crustal assimilation. *Journal of Volcanology and Geothermal
Research*, 206, 136–147.

Fraser, G. S., DeCelles, P. G., 1992. Geomorphic controls on sediment accumulation at
margins of foreland basins. *Basin Research*, 4, 233-252.

Gangui A, Götze, H.J., 1996. The Deep Structure of the Northern Puna (Argentina) -
Constraints from 2D Seismic Data and 3D Gravity Modelling. XIII Congreso Geológico
Argentino, Proceedings II, 545-565, Buenos Aires.

Guzmán, S., I.A. Petrinovic, J.A. Brod, F.D. Hongn, R.E. Seggiaro, C. Montero, R.
Carniel, E.L. Dantas, M. Sudo, 2011. Petrology of the Luingo caldera (SE margin of the
Puna plateau): A middle Miocene window of the arc–back arc configuration. *J.
Volcanol. Geo Res.*, 200 (3-4), 171-191.

1
2
3
4
5
6
7
8
9
10
11
12
13
14
15
16
17
18
19
20
21
22
23
24
25
26
27
28
29
30
31
32
33
34
35
36
37
38
39
40
41
42
43
44
45
46
47
48
49
50
51
52
53
54
55
56
57
58
59
60
61
62
63
64
65

Hongn, F. Tubía, J.M., Aranguren, A., Mon, R., 2002. La monzodiorita Las Burras: un plutón Mioceno en el Batolito de Tastil, Cordillera Oriental Argentina. XV Congreso Geológico Argentino, Proceedings, II, 128-133, Calafate.

Hongn, F., del Papa, C., Powel, J., Petrinovic, I.A., Mon, R., Deraco, V., 2007. Middle Eocene deformation and sedimentation in the Puna-Eastern Cordillera transition (23°–26° S): Inheritance of preexisting anisotropies on the pattern of initial Andean shortening. *Geology*, 35 (3), 271-274.

Hongn, F., Mon, R., Petrinovic, I., del Papa, C., Powell, J., 2010. Inversión y reactivación tectónicas cretácico-cenozoicas en el noroeste argentino: influencia de las heterogeneidades del basamento neoproterozoico-paleozoico inferior. *Revista de la Asociación Geológica Argentina*, 66(1), 38-53.

Hongn F., del Papa C., Powell J., Payrola P., Petrinovic I., Mon R. 2011. Fragmented Paleogene foreland basin in the Valles Calchaquíes, NW of Argentina. In: J.A., Salfity & R.A. Marquillas (Eds) *Cenozoic Geology of the Central Andes of Argentina*. SCS Publisher, Salta, 189-209.

Insel, N., Grove, M., Haschke, M., Barnes, J.B., Schmitt, A.K., Strecker, M.R., 2012. Paleozoic to early Cenozoic cooling and exhumation of basement underlying the eastern Puna Plateau margin prior to plateau growth. *Tectonics*, 31, TC6006, doi:10.1029/2012TC003168.

Lanza, F., Tibaldi, A., Bonali, F.L., Corazzato, C., 2013. Space–time variations of stresses in the Miocene–Quaternary along the Calama–Olacapato–El Toro Fault Zone, Central Andes. *Tectonophysics* 593, 33–56.

Llambías, J.E., Sato, A.M., Tomsic J., 1985. Geología y características químicas del stock terciario del Nevado de Acay y vulcanitas asociadas. *Revista Asoc. Geol. Arg.*, 40 (3- 4), 158-176.

Jan, A., Cooker, M. J. 2016. Moving boulders in flash floods and estimating flow conditions using boulders in ancient deposits. *Sedimentology*, doi: 10.1111/sed.12274.

JICA, 1993. Informe sobre Exploración de Minerales del área Oeste de la República Argentina. Fase I (Marzo 1993) NE17. Metal Mining Agency of Japan.

Jordan, T., 1995. Retroarc Foreland and Related Basins. In: Busby, C.E. & R.V. Ingersoll (Eds) *Tectonics of Sedimentary Basins*. Blackwell Sciences, pp 579. Cambridge.

1
2
3
4
5
6
7
8
9
10
11
12
13
14
15
16
17
18
19
20
21
22
23
24
25
26
27
28
29
30
31
32
33
34
35
36
37
38
39
40
41
42
43
44
45
46
47
48
49
50
51
52
53
54
55
56
57
58
59
60
61
62
63
64
65

Marrett, R., Allmendinger, R. Alonso, R., Drake, R., 1994. Late Cenozoic tectonic evolution of the Puna Plateau and adjacent foreland, northwestern Argentine Andes. *Journal of South American Earth Sciences*, 7, 179-207.

Mazzuoli, R., Vezzoli, L., Omarini, R., Acocella, V., Gioncada, A., Matteini, M., Dini, A., Guillou, H., Hauser, N. Uttini, A., Scaillet, S., 2008. Miocene magmatism and tectonics in the easternmost sector of the Calama-Olacapato-El Toro fault system in Central Andes at ~24°S: Insights into the evolution of the Eastern Cordillera. *Geol. Soc. Am. Bull.*, 120, 1493-1517.

Méndez, V., Navarini, A., Piazza, D., Viera, O., 1973. Faja eruptiva de la Puna Oriental. V Congreso Geológico Argentino, Villa Carlos Paz, Proceedings, IV, 89-100.

Nemec, W., Steel, R.J., 1984. Alluvial and coastal conglomerates: their significant features and some comments on gravelly mass-flow deposits. In: Koster E.H. & Steel R.J. (Eds), *Sedimentology of gravel and conglomerates*. Canadian Soc. Petrol. Geol. Mem., 10, 1-31.

Norini, Báez, G. W., Becchio, R., Viramonte, J., Giordano, G., Arnosio, M., Pinton, A. and Gropelli, G., 2013. The Calama-Olacapato-El Toro fault system in the Puna plateau, Central Andes: Geodynamic implications and stratovolcanoes emplacement. *Tectonophysics*, DOI: 10.1016/j.tecto.2013.06.013.

Payrola Bosio P.A., Powell J., del Papa C., Hongn F., 2009. Middle Eocene deformation-sedimentation in the Luracatao Valley: Tracking the beginning of the foreland basin of Northwestern Argentina. *Journal of South America Earth Sciences*, 28, 142-154.

Petrinovic, I. A., Mitjavila, J., Viramonte, J.G., Martí, J., Becchio, R., Arnosio, M., Colombo, F., 1999. Descripción geoquímica y geocronológica de secuencias volcánicas neógenas de Trasarco, en el extremo oriental de la Cadena Volcánica Transversal del Quevar (Noroeste de Argentina). In: Colombo, F., Queralt, I. and Petrinovic, I.A. (Eds). *Geología de los Andes Centrales Meridionales: El Noroeste Argentino*, Acta Geologica Hispánica, 34, 255-272.

Petrinovic, I.A., Riller, U., Brod, A., 2005. The Negra Muerta volcanic complex, southern Central Andes: geochemical characteristics and magmatic evolution of an episodic volcanic centre. *J. of Volcanol. and Geo. Res.*, 140 (4), 295-320.

Petrinovic, I.A., Riller, U., Alvarado, G., Brod, J.A, Arnosio, M., 2006. Bimodal volcanism in a tectonic transfer zone: evidence for tectonically controlled magmatism in

1 the southern Central Andes, NW Argentina. *J. of Volcanol. and Geo. Res.*, 152, 240-
2 252.

3 Petrinovic, I.A., Marti J., Aguirre-Diaz G.J., Guzmán S., Geyer A., Salado Paz N.,
4 2010. The Cerro Aguas Calientes caldera, NW Argentina: an example of a tectonically
5 controlled, polygenetic collapse caldera, and its regional significance. *J. Volcanol. Geo.*
6 *Res.* doi.org/10.1016/j.jvolgeores.2010.04.012

7 Ramos, V., 1973. Estructura de los primeros contrafuertes de la Puna salto-jujeña y sus
8 manifestaciones volcánicas asociadas 5° Congreso Geológico Argentino, Proceedings 4,
9 159-202. Córdoba.

10 Reijs, J., McClay, K., 1998. Salar Grande pull-apart basin, Atacama fault system,
11 northern Chile. In Holdsworth, R.E., Strachan, R.A., and Dewey, J.F., (Eds.),
12 Continental transpressional and transtensional tectonics. London, Geological Society
13 Special Publication, 135, 127–141.

14 Reiners, P.W., S.N. Thomson. A. Vernon, S.D. Willett, M. Zattin, J. Einhorn, G.
15 Gehrels, J. Quade, D. Pearson, K.E. Murray, W. Cavazza, 2015. Low-temperature
16 thermochronologic trends across the central Andes, 21°S–28°S. In: P.G. DeCelles, M.N.
17 Ducea, B. Carrapa and P.A. Kapp (Eds.), *Geodynamics of a Cordilleran Orogenic*
18 *System, The Central Andes of Argentina and Northern Chile*. Geological Society of
19 America Memoir, 212, doi,10.1130/2015.1212(15).

20 Riller, U., Greskowiak, J., Ramelow, J., Strecker, M., 1999. Dominant modes of
21 Andean deformation in the Calchaquí River Valley, NW-Argentina. 14° Congreso
22 Geológico Argentino, proceedings 1, 201-204. Salta.

23 Riller, U., Petrinovic, I., Ramelow, J., Greskowiak, J., Strecker, M., Oncken O., 2001.
24 Late Cenozoic tectonism, caldera and plateau formation in the central Andes. *Earth and*
25 *Planetary Science Letters* 188, 299-311.

26 Riller, U. and O. Oncken, 2003. Growth of the Central Andean plateau by tectonic
27 segmentation is controlled by the gradient in crustal shortening. *The Journal of Geology*
28 111: 367-384.

29 Salado Paz, N., Petrinovic, I.A., Avila, J., Brod, A. 2016. Geología, mineralogía y
30 estructura de la mina Acazoque (Pb-Ag-Zn), Puna salteña. *Revista de la*
31 *Asociación Geológica Argentina* 73, in press.

32 Salfity, J. A., Gorustovich, S. Moya, C., Amengual, R., 1984. Marco tectónico de la
33 sedimentación y efusividad cenozoicas en la Puna argentina. 9° Congreso Geológico
34 Argentino, Proceedings 1, 539-554. Bariloche.

35
36
37
38
39
40
41
42
43
44
45
46
47
48
49
50
51
52
53
54
55
56
57
58
59
60
61
62
63
64
65

1 Santimano, T., Riller, U., 2012. Kinematics of Tertiary to Quaternary intracontinental
2 deformation of upper crust in the Eastern Cordillera, southern Central Andes, NW
3 Argentina. *Tectonics*, 31, TC4002, doi:10.1029/2011TC003068.
4
5 Schwab, K., Lippolt, H., 1974. K-Ar mineral Ages and Late Cenozoic History of the
6 Salar de Cauchari area (Argentina Puna). *Andean and Antarctic Volcanologic problems*,
7 Santiago, 698-715.
8
9 Seggiaro, R. 2006. Variaciones estructurales a lo largo del lineamiento Calama–
10 Olacapato–Toro en el noroeste argentino. XI Congreso Geológico Chileno,
11 proceedings 1, 337–340.
12
13 Strecker, M.R., Alonso, R.N., Bookhagen, B., Carrapa, B., Hilley, G.E., Sobel, E.R.,
14 Trauth, M.H., 2007. Tectonics and climate of the Southern Central Andes. *Annual*
15 *Review of Earth and Planetary Sciences* 35, 747–787.
16
17 Suzaño, N.O., Becchio, R.A., Sola, A., Arnosio, M., Nieves, A.I., 2015. Geología del
18 prospecto Vicuña Muerta: emplazamiento múltiple y control estructural de cuerpos
19 subvolcánicos miocenos en el borde oriental de la Puna Austral, Salta. *Revista de la*
20 *Asociación Geológica argentina* 72, in press.
21
22 Turner J. C. M., 1960. Estratigrafía de la Sierra de Santa Victoria y adyacencias.
23 *Academia Nacional de Ciencias de Córdoba Bulletin* 41, 163-196.
24
25 Viramonte, J.G., Galliski, M.A., Araña Saavedra, V., Aparicio, A., Cacho, G.L., Parica,
26 C., 1984. Edad, génesis y mecanismos eruptivos de las riolitas granatíferas de San
27 Antonio de los Cobres, provincia de Salta. IX Congreso Geológico Argentino,
28 proceedings III, 216-233. Bariloche.
29
30
31
32
33
34
35
36
37
38
39
40
41

42 **FIGURE CAPTIONS**

43
44
45 Figure 1. A. Regional map of major structures and outcrops of the units described in the
46 text. B. Local map of outcrops and main structures at Corte Blanco. Modified from
47 Donato and Vergani (1988); Blasco et al. (1996); Petrinovic et al. (1999); Arnosio
48 (2002); Riller et al. (2001).
49
50
51

52
53 Figure 2: Stratigraphic relations of the Conglomerado Los Patos with the underlying
54 and overlying units in the Corte Blanco area. MG: Maíz Gordo, Me: Mealla formations.
55
56

57 Figure 3: Sedimentological log and provenance of the Conglomerado Los Patos at Corte
58 Blanco.
59
60
61
62
63
64
65

1
2
3
4
5
6
7
8
9
10
11
12
13
14
15
16
17
18
19
20
21
22
23
24
25
26
27
28
29
30
31
32
33
34
35
36
37
38
39
40
41
42
43
44
45
46
47
48
49
50
51
52
53
54
55
56
57
58
59
60
61
62
63
64
65

Figure 4: Sedimentary lithofacies and clast compositions. A. Gmm facies at the basal section. B. Boulder clasts of Miocene volcanics (v) and schist (sch). C. Cobble-sized clast of Gmm facies. Qs: quartz arenite, Phy: phyllite, Sch: schist. D. Gch facies, note the organized aspect respect to Gmm facies, outcrop is 9 meters. E. Close-up view of Gch facies, cobble-rich and pebble-rich pair layers. F. Gci facies, note the well-organized deposit and the imbricated clasts.

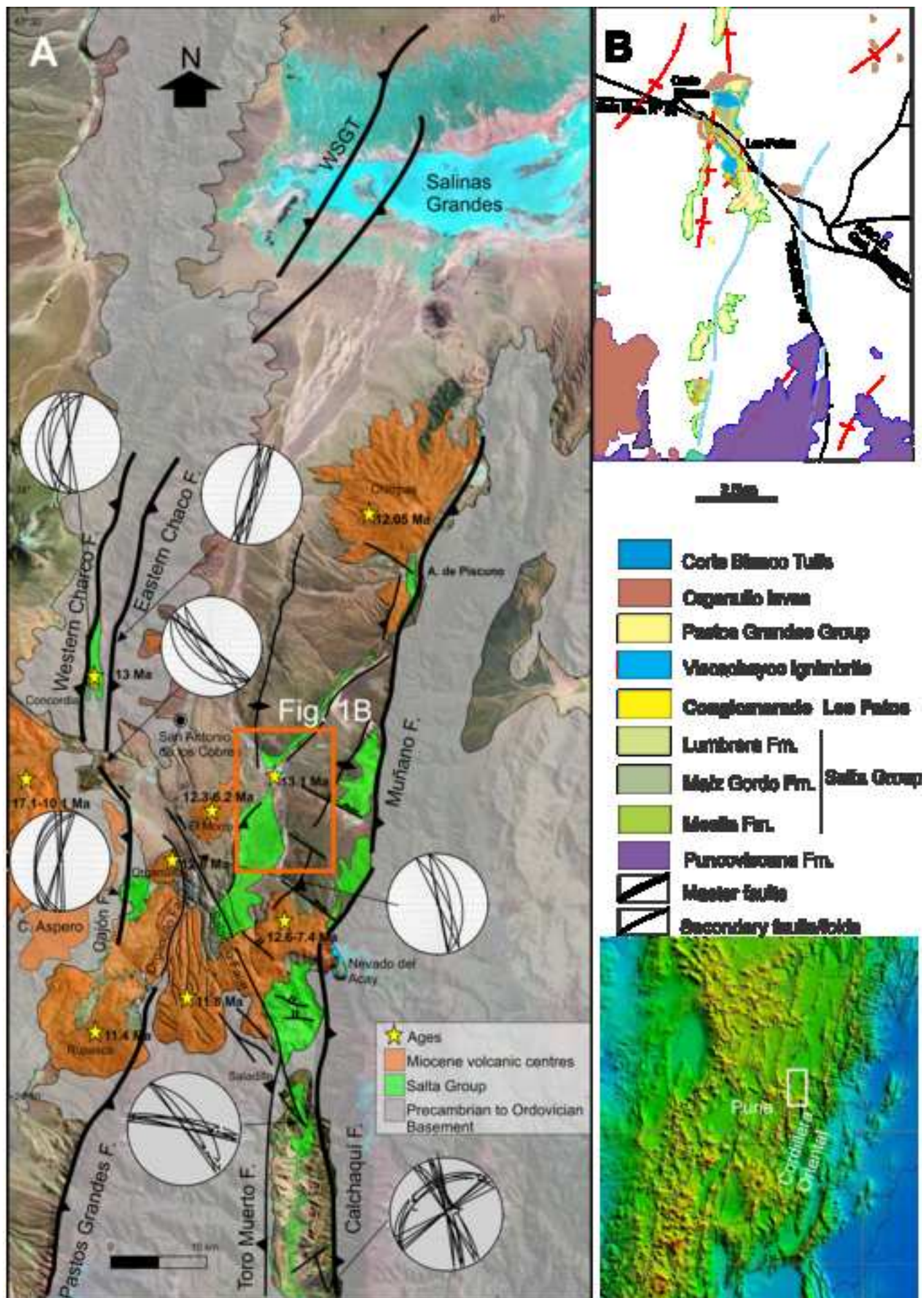
Figure 5: U/Pb radiometric determinations in zircons from volcanic clasts in the lower section of the Conglomerado Los Patos (see Fig. 3). Methodology and characteristics are explained in the text.

Figure 6: a) Muñano Fault; b) breccia fault in conglomeratic deposits of the Salta Group, Quebrada de Piedra Caída; c) Charco Oriental Fault, mineralized breccia; d) Saladillo Fault (recumbent fold in Salta Group). Dotted lines indicate the approximate dipping of the fault plane.

Figure 7: Structural interpretation scheme of the Calchaquí and San Antonio de los Cobres valleys, the topographic position of the interpreted tectonic transfer zone (DEM: SRTM 30m). Red stars indicate the location of the Miocene eruptive centers.

Table 1: Structural data (graphs in Fig. 1A). Rb: strike; Bz: Dip; C: quadrant dip; PE: striae plane; IE: Striae dip; M: relative movement of blocks; Q: quality (1-4); Lat / Lon: geographical coordinates of the stations.

Figure
[Click here to download high resolution image](#)



Figure

[Click here to download high resolution image](#)

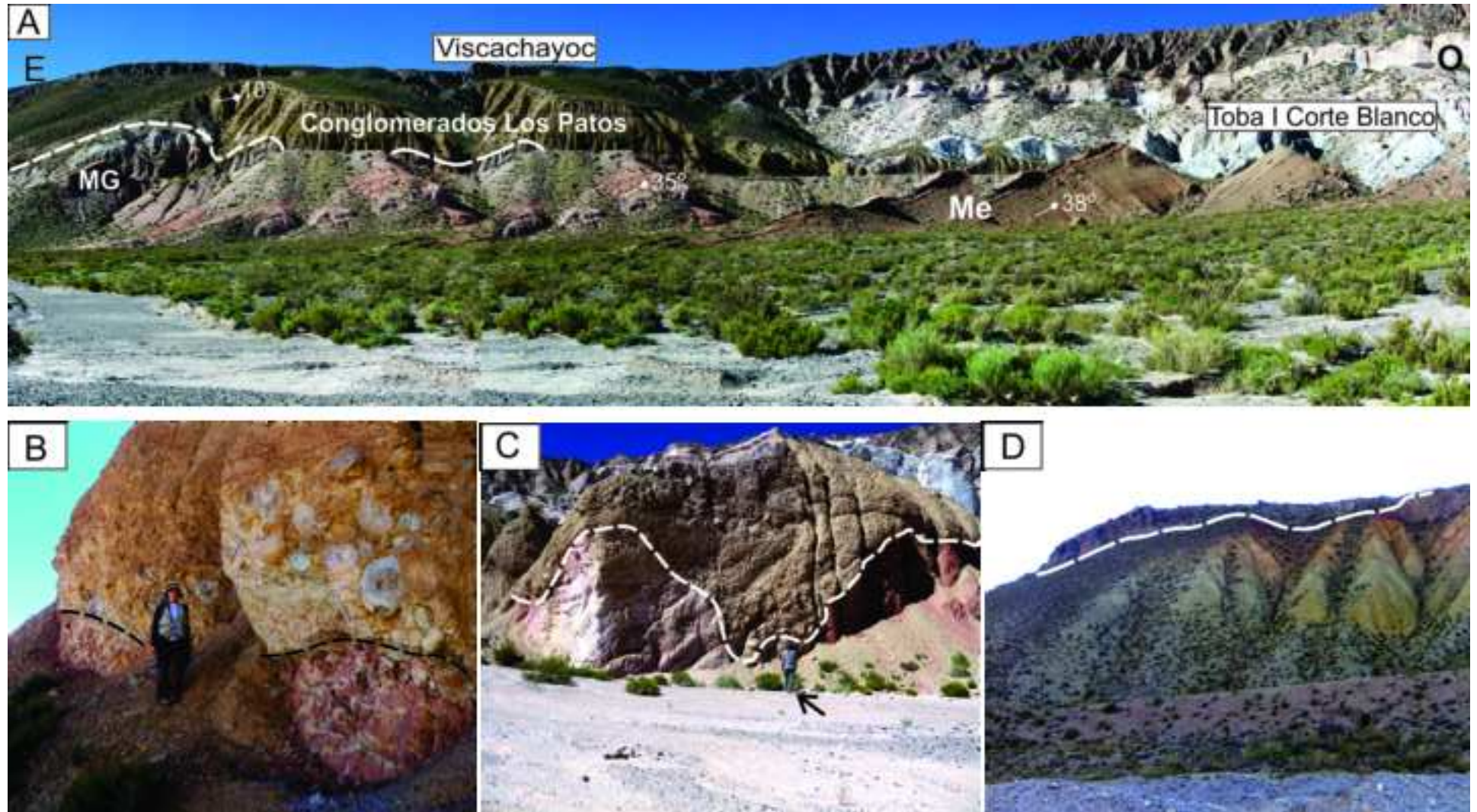


Figure
[Click here to download high resolution image](#)

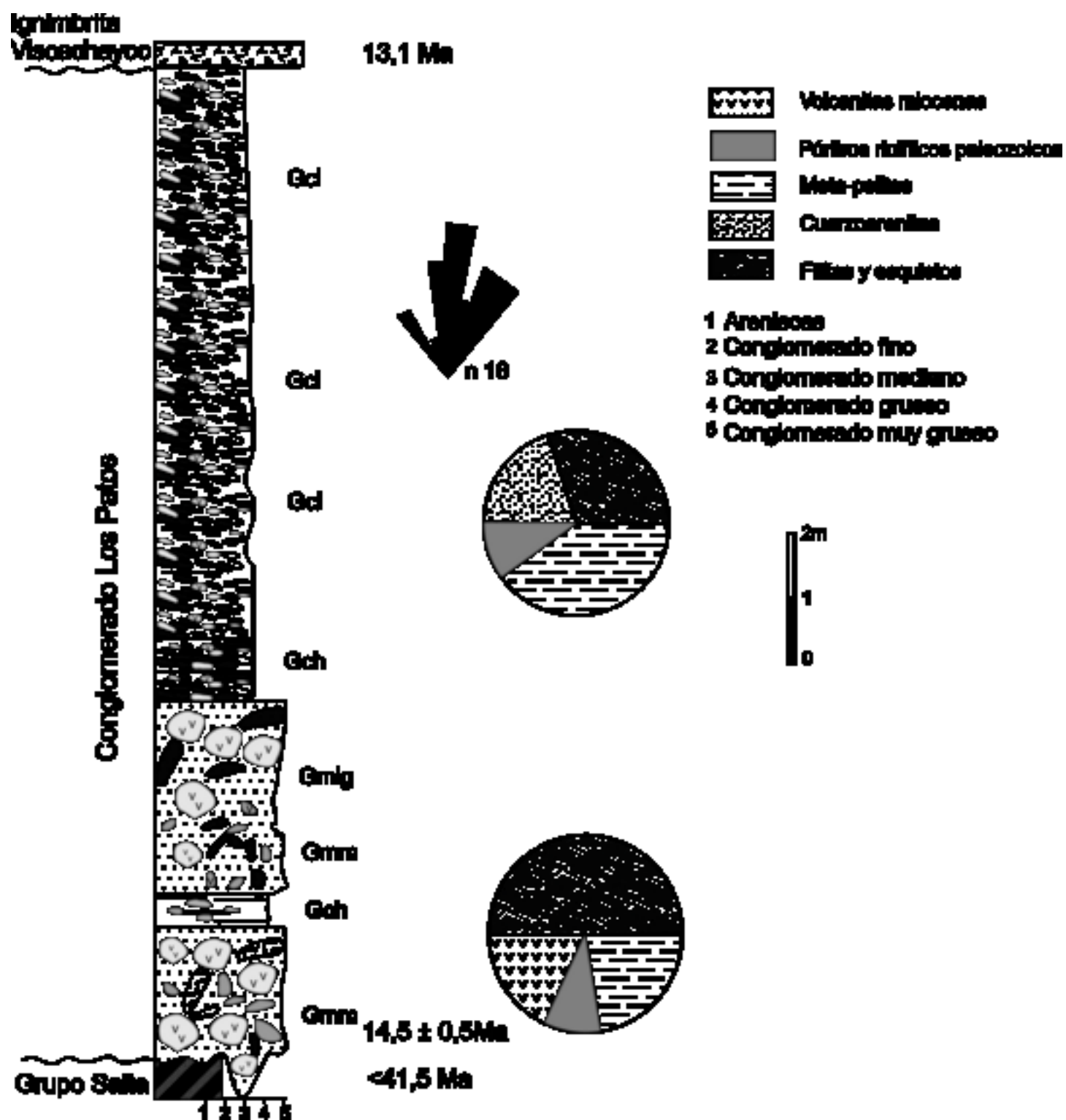
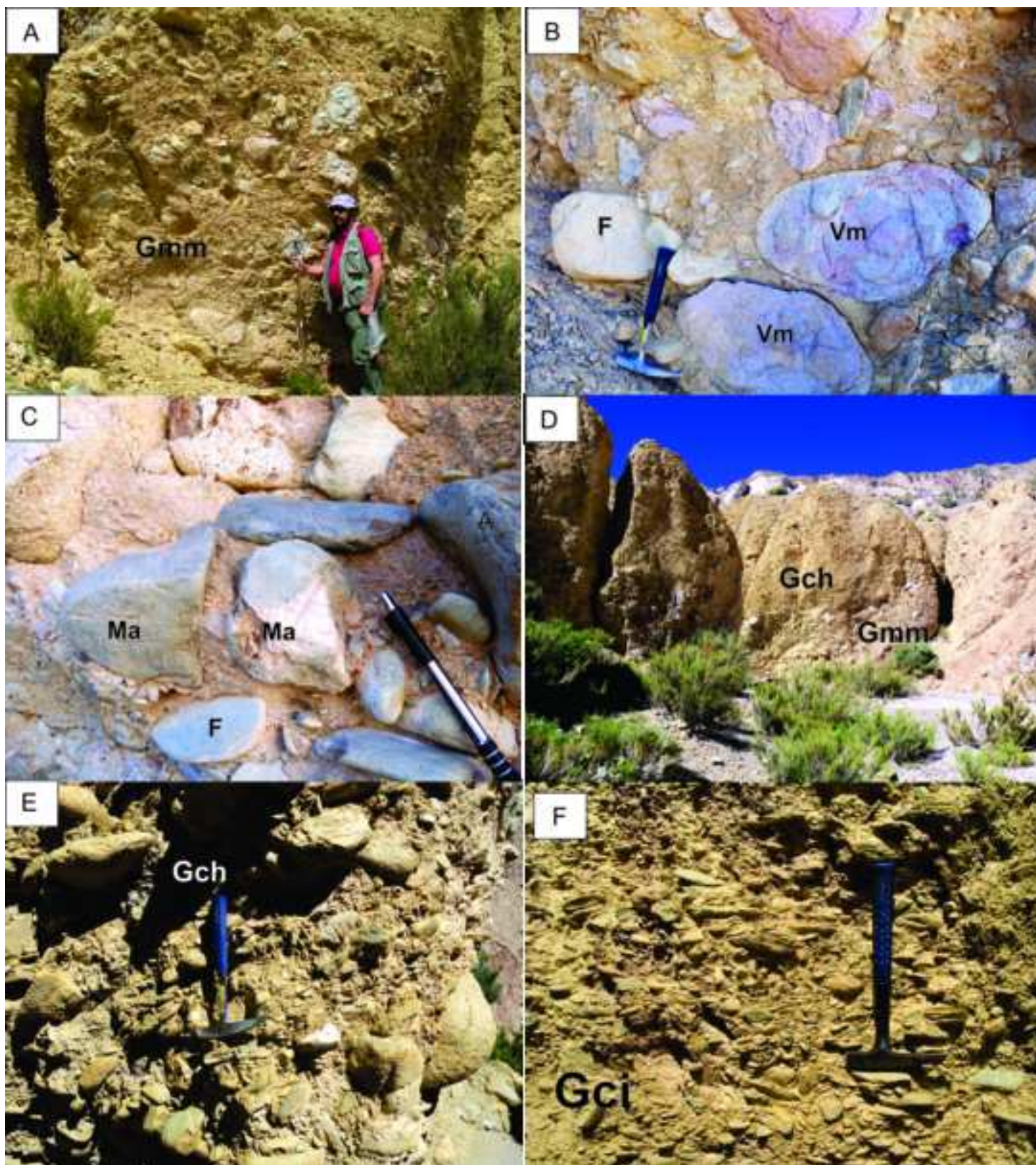
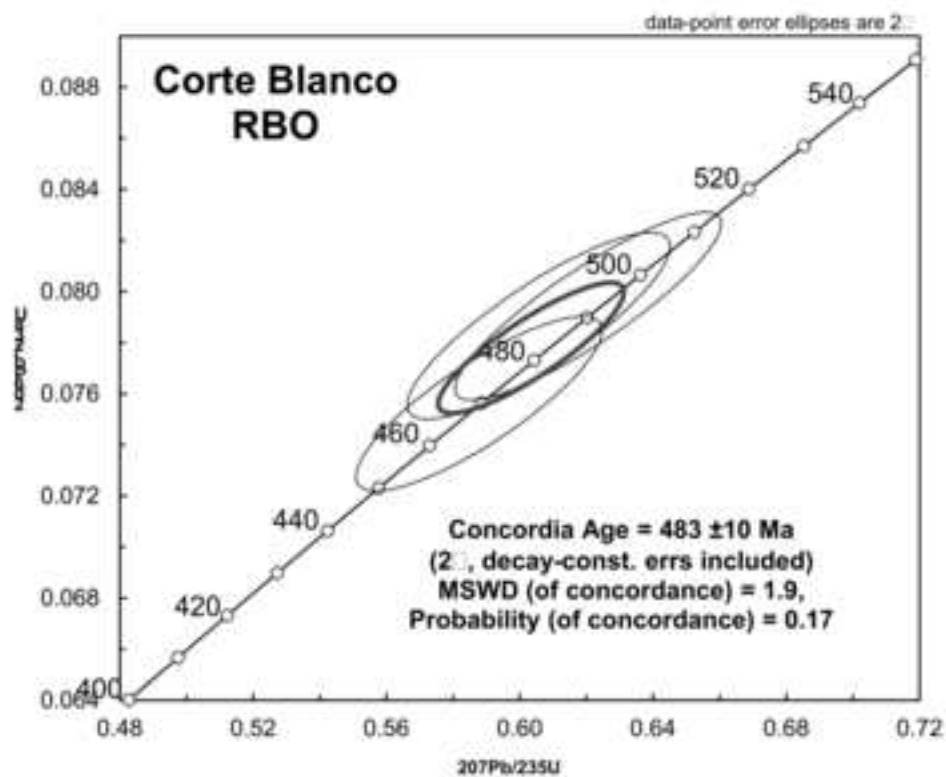
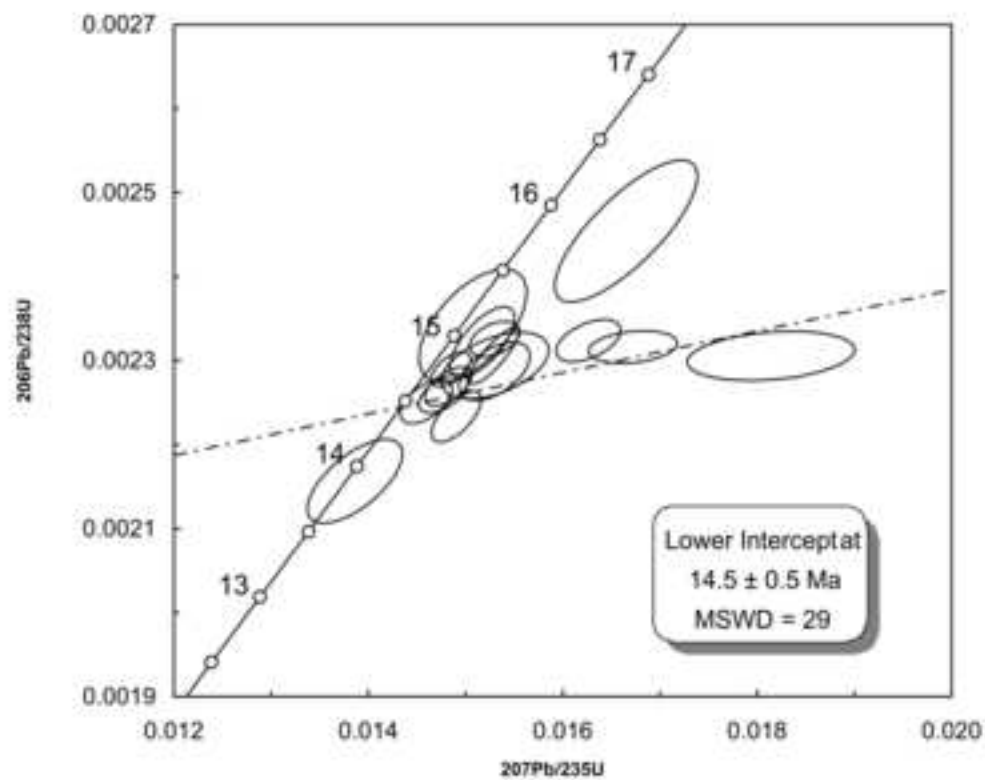


Figure
[Click here to download high resolution image](#)



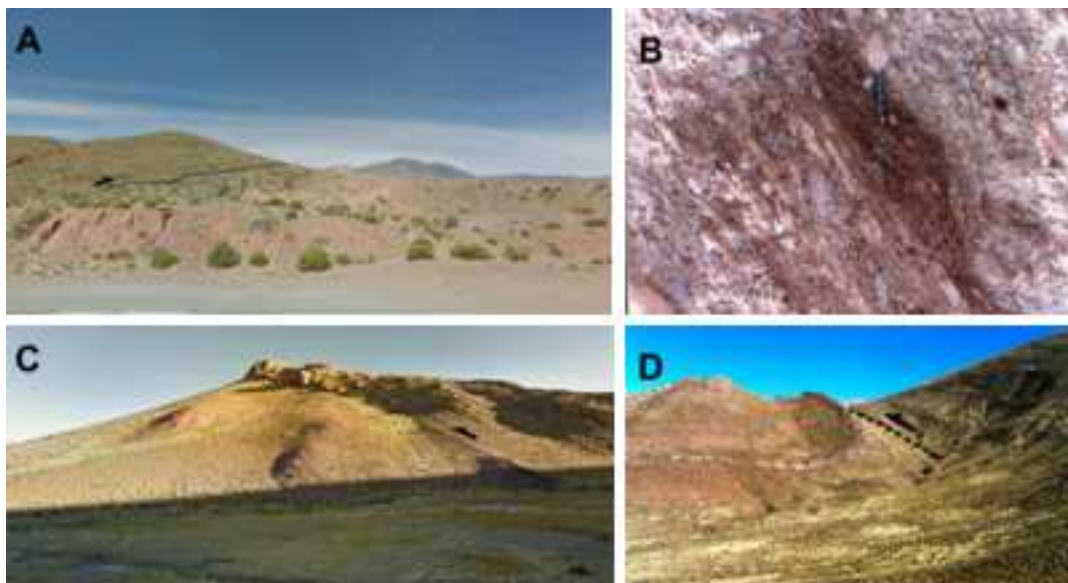
Figure

[Click here to download high resolution image](#)



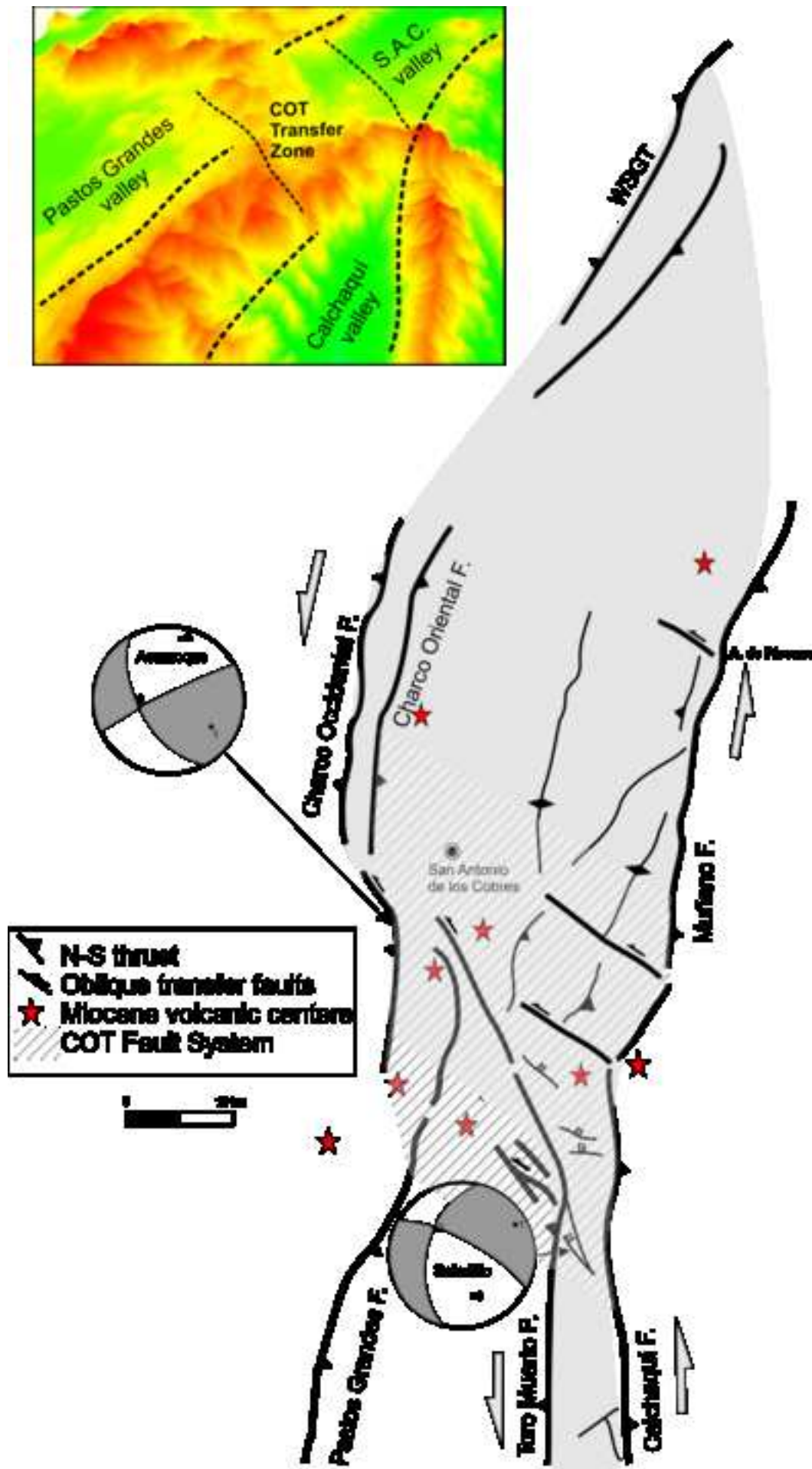
Figure

[Click here to download high resolution image](#)



Figure

[Click here to download high resolution image](#)



Table

1
2
3
4
5
6
7
8
9
10
11
12
13
14
15
16
17
18
19
20
21
22
23
24
25
26
27
28
29
30
31
32
33
34
35
36
37
38
39
40
41
42
43
44
45
46
47
48
49
50
51
52
53
54
55
56
57
58
59
60
61
62
63
64
65

Station	S	D	Q	PS	SD	M	Q	Lat	Lon
Acazoque	200	55	W			R	3	24°23'4.83"S	66°20'27.49"O
	185	48	W			R	3	24°23'4.83"S	66°20'27.49"O
	196	51	W			R	3	24°23'4.83"S	66°20'27.49"O
	178	49	W			R	3	24°23'4.83"S	66°20'27.49"O
Chorrillos	130	65	S			R	2	24°16'10.73"S	66°23'25.06"O
	130	40	S			R	2	24°16'10.73"S	66°23'25.06"O
	135	72	S			R	2	24°16'10.73"S	66°23'25.06"O
	148	74	W			R	2	24°16'10.73"S	66°23'25.06"O
Gemelos	342	81	E	82	80	N	1	24°45'2.61"S	66°10'8.02"O
	325	76	E	63	75	N	2	24°45'2.61"S	66°10'8.02"O
	233	37	S	292	32	R	2	24°45'2.61"S	66°10'8.02"O
	246	39	S	295	31	R	2	24°45'2.61"S	66°10'8.02"O
	345	81	E	68	80	R	1	24°45'2.61"S	66°10'8.02"O
	330	75	E	72	74	N	3	24°45'2.61"S	66°10'8.02"O
	352	86	E	68	85	R	3	24°45'2.61"S	66°10'8.02"O
	230	45	S	278	36	R	2	24°45'2.61"S	66°10'8.02"O
Organullo	238	48	S	40	18	N	2	24°45'2.61"S	66°10'8.02"O
	335	75	E				2	24°19'12.45"S	66°19'35.23"O
	350	50	E				2	24°19'12.45"S	66°19'35.23"O
Saladillo	350	70	E				2	24°19'12.45"S	66°19'35.23"O
	278	75	E	87	35	N	1	24°33'32.80"S	66°12'13.29"O
	325	78	E	132	45	N	2	24°33'32.80"S	66°12'13.29"O
	322	60	E	133	15	R	3	24°33'32.80"S	66°12'13.29"O
	282	80	E	94	35	N	2	24°33'32.80"S	66°12'13.29"O
	285	78	E	93	44		4	24°33'32.80"S	66°12'13.29"O